ARTICLE

OBC
www.rsc.org/obc

Multifunctional redox catalysts as selective enhancers of oxidative stress

Fiona H. Fry,†[a] Andrea L. Holme,†[a] Niroshini M. Giles,[a] Gregory I. Giles,[a] Catriona Collins,[a] Kim Holt,[a] Sandra Pariagh,[a] Thomas Gelbrich,[b] Michael B. Hursthouse,[b] Nick J. Gutowski[c] and Claus Jacob*[a,d]

[a] *School of Biological and Chemical Sciences, University of Exeter, Stocker Road, Exeter, UK EX4 4QD*

[b] *School of Chemistry, University of Southampton, Highfield, Southampton, UK SO17 1BJ*

[c] *Peninsula Medical School, Universities of Exeter and Plymouth and The Royal Devon and Exeter Hospital, Exeter, UK EX2 5DW*

[d] *Fachbereich 8.2 Pharmazeutische und Medizinische Chemie, Universität des Saarlandes, Postfach 151150, D-66041, Saarbrücken, Germany. E-mail: c.jacob@mx.uni-saarland.de; Fax: +49 (0)681 302 4386; Tel: +49 (0)681 302 2424*

Received 11th February 2005, Accepted 20th May 2005
First published as an Advance Article on the web 9th June 2005

Certain cancer cells proliferate under conditions of oxidative stress (OS) and might therefore be selectively targeted by redox catalysts. Among these catalysts, compounds containing a chalcogen and a quinone redox centre are particularly well suited to respond to the presence of OS. These catalysts combine the specific electrochemical features of quinones and chalcogens. They exhibit high selectivity and efficiency against oxidatively stressed rat PC12, human Jurkat and human Daudi cells in cell culture, where their mode of action most likely involves the catalytic activation of existent and the generation of new reactive oxygen species. The high efficiency and selectivity shown by these catalysts makes them interesting for the development of anti-cancer drugs.

Introduction

Several cancer cells, such as the cells of lung, kidney and prostate cancer, possess significantly elevated intracellular levels of reactive oxygen species (ROS).[1–2] The latter include, among others, the superoxide anion radical ($O_2^{\bullet -}$), the hydroxyl radical ($^{\bullet}OH$), hydrogen peroxide (H_2O_2), organic peroxides and radicals and singlet molecular oxygen.[3] In healthy cells, the concentration of these chemical species is low and increases in the level of ROS, that are within the micromolar range for some stressors, can be seen as good diagnostic markers of OS related diseases.[4–5] We have recently proposed that compounds able to use these naturally occurring ROS markers to kill cells could possess an interesting combination of sensor and effector properties that might make them selective in targeting oxidatively stressed cells.[6–8] Within this context, we have shown that catalytic agents mimicking redox enzymes such as glutathione peroxidase (GPx) are particularly good candidates, since they combine selectivity for their natural (ROS) substrate(s) with high (catalytic) efficiency at low doses.[6–8]

Among such catalysts, multifunctional compounds able to respond to a range of oxygen species are of special interest, since they can take full account of the complex cellular redox environment existing during OS. Preliminary studies in cultured mammalian PC12 cells have already shown that compounds integrating two redox groups, *i.e.* a redox active quinone and a chalcogen moiety, are particularly suited to discriminate between oxidatively stressed and unstressed cells in culture and that some catalysts are active in concentrations below 1 μM.[6–8] At the time, however, the ability of such catalysts to effectively and selectively kill cells under OS was only demonstrated for undifferentiated rat PC12 cells and the precise redox behaviour and mode of action of these compounds remained largely unexplored.

Here we present a more comprehensive study of the activities of such catalysts *in vitro* and in different bioassays, including a detailed account of the synthesis and electrochemical analysis of the compounds. Importantly, we also show that the sensor–effector properties of such redox catalysts are not limited to PC12 cells, but are also observed in human Jurkat and Daudi cell lines and that the probable mode of action of the catalysts involves an increase in levels of intracellular OS.

Results

Selection and synthesis of multifunctional catalysts

Compounds **1–4** (Fig. 1) were chosen since they combine two individual redox systems, *i.e.* a quinone and a chalcogen, in one molecule, which should allow them to participate in a broad spectrum of redox reactions. The compounds were then studied in a range of assays, with the aim to gain a more comprehensive understanding of their chemical and biochemical properties, biological activities and potential mode(s) of action inside cells.

While the electrochemical studies confirmed the presence of two individual redox centres in these molecules, the *in vitro* catalytic assays indicated the ability of **2–4** to participate in catalytic peroxidation and radical generation reactions. The activity of the catalysts was therefore evaluated in cell culture and the anticipated cytotoxic effects in the presence of peroxide were observed not only in the rat PC12 cell line, but also in human Jurkat and Daudi cell lines. Further evaluation with intracellular, fluorescent redox indicators resulted in preliminary biochemical results pointing towards a (catalytic) increase of intracellular OS, with apoptotic cell death as the probable mode of action of these catalytic compounds.

The following paragraphs describe the results obtained in the structural, electrochemical, biochemical and cell culture studies of **1–4** in more detail.

Structural and electrochemical analysis

Structural analysis was employed to ensure the presence and correct configuration of the quinone and chalcogen redox centres. The X-ray crystal structure of tellurium compound **3**

† These authors contributed equally.

DOI: 10.1039/b502197a

Table 1 Electrochemical parameters of **1–5**.[6] Potentials for the quasi-reversible quinone redox couple (Epa$_1$ and Epc) and the irreversible chalcogen oxidation (Epa$_2$) at pH = 7.4 are provided. pH-Dependence of the oxidation and reduction potentials plays a major role in the pH control of the redox activity of the compounds. $\Delta E/\Delta$pH values were determined between pH 4 and pH 9. Experimental details are given in the text. Experimental error ±10 mV

Compound	Quinone Epa$_1$/mV	Quinone Epc/mV	Quinone $E_{\frac{1}{2}}$/mV	Chalcogen Epa$_2$/mV	ΔEpa$_1$/ΔpH/mV	ΔEpc/ΔpH/mV	ΔEpa$_2$/ΔpH/mV
1	−70	−302	−186	+1348	−89	−89	+13
2	−57	−328	−193	+1128	−71	−42	+7
3	−115	−341	−228	+823	−73	−40	[a]
4	−116	−341	−229	+760	−75	−40	[a]
5	−166	−277	−222	—	−76	−38	—

[a] For **3** and **4**, Epa$_2$ decreases from pH 4 to 7.4 with ΔEpa$_2$/ΔpH = −41 mV and −62 mV, respectively. Epa$_2$ increases from pH 7.4 to 9 with ΔEpa$_2$/ΔpH = +120 mV and +187 mV, respectively.

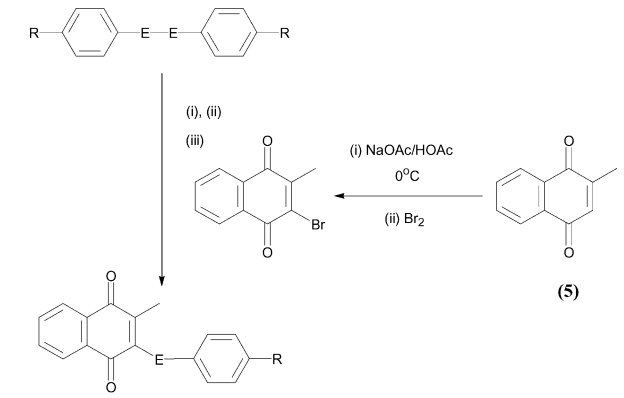

Compound	E	R
1	S	OCH_3
2	Se	OCH_3
3	Te	H
4	Te	OCH_3

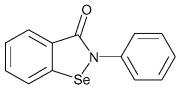

Ebselen

Fig. 1 Synthesis and chemical structures of multifunctional compounds used in this study. For E = Se: (i) Bu_3P–THF–argon; (ii) NaOH. For E = S, Te: (i) $NaBH_4$–EtOH–argon; (ii) not applicable. Details of the chemical synthesis are described in the text. The structure of ebselen is given as a comparison.

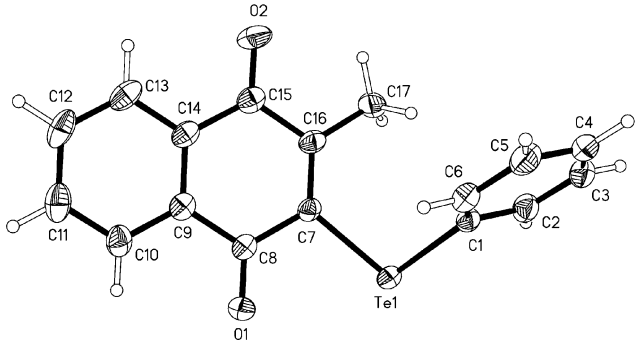

Fig. 2 Molecular structure of **3**. Selected bond lengths (Å) and angles (°): Te1–C1 = 2.124(3) and Te1–C7 = 2.119(3) Å; C1–Te–C7 = 96.64(13) Å.

was successfully solved‡ and is shown in Fig. 2. This structure confirms the close proximity of the quinone and tellurium redox centres. The Te–C bond lengths (Te1–C1 = 2.124(3) Å and Te1–C7 = 2.119(3) Å) and the bond angle centred on the tellurium (C1–Te–C7 = 96.64(13)°) are in good agreement with literature values, indicating a normal fusion of the two parts of the molecule.[9–10]

‡ CCDC reference number 269419. See http://www.rsc.org/suppdata/ob/b5/b502197a/ for crystallographic data in CIF or other electronic format.

The two redox centres in **1–4** were then analysed by cyclic voltammetry. The latter provides insight into the oxidation and reduction processes such compounds might participate in, both *in vitro* and *in vivo*.[6,11,12] We have recently communicated preliminary electrochemical results for **1–4**.[6] In short, these compounds exhibited a combination of two distinct redox behaviours indicative of one quinone and one chalcogen centre (Table 1). At pH 7.4, the quinone redox couple (Epa$_1$ and Epc) appeared at around −200 mV *vs.* SSE, with quasi-reversible characteristics, such as a peak current ratio ($|I$pa$_1/I$pc$|$) ≈ 0.7 and transfer coefficients for $\alpha_c n_\alpha$ between 0.9 (**3**) to 1.0 (**4**) and for $\alpha_a n_\alpha$ between 0.6 (**3**) to 0.7 (**4**). Assuming a (standard) value of 0.5 for α, this would imply n_α values of 1.8 for the reduction peak and 1.4 for the oxidation peak, *i.e.* approximately two electrons transferred during reduction of the quinone to the dihydroquinone and between one and two during subsequent oxidation to the semiquinone and quinone, respectively.[6]

The quinone redox centre in **1–4** was under pH control (Table 1). Both Epa$_1$ and Epc values of **1–5** consistently decreased between pH 4 and 9, with ΔEpa$_1$/ΔpH ≈ −75 mV for **1–5** and ΔEpc/ΔpH ≈ −40 mV for **1–5**. These results imply a shift of the oxidation and reduction potentials of the quinone moiety to more reducing potentials upon an increase of the pH. From a chemical perspective this is hardly surprising, since the reduction of the quinone to semi- and dihydroquinone involves a protonation step at oxygen, while oxidation to quinone involves a deprotonation step. Deprotonation of the OH-group at higher pH values therefore makes the semi- and dihydroquinone forms more reducing.

The chalcogen centre resulted in an irreversible oxidation peak (Epa$_2$) between +760 mV (**4**) and +1350 mV (**1**).[6] In agreement with previous studies, the sulfur compound (**1**) exhibited the highest oxidation potential and the tellurium compounds **3** and **4** the lowest. Electron withdrawing effects of the quinone led to more positive oxidation potentials for the chalcogen atoms in **2** and **4** when compared to their previously studied symmetrical 4,4′-dimethoxydiphenyl selenide (Epa = +753 mV) and 4,4′-dimethoxydiphenyl telluride (Epa = +368 mV) analogues.[6]

Chalcogen oxidation in **1–4** was also under pH control. Unlike the quinone oxidation and reduction potentials for **1** and **2**, chalcogen oxidation potentials increased with increasing pH, albeit with considerably smaller changes (ΔEpa$_2$/ΔpH = 13 mV for **1** and 7 mV for **2**). The pH-dependency of Epa$_2$ of the tellurium compounds **3** and **4** was more complex, with an initial decrease in Epa$_2$ with between pH 4 and 7.4 followed by a sharp increase between pH 7.4 and 9 (Table 1). This somewhat different redox behaviour of tellurium compounds **3** and **4**, when compared with the sulfur and selenium analogues, might be related to their high activity in the PhSH and MT assays. Tentatively, an Epa$_2$ minimum at around 7.4 would imply highest peroxidation activity of **3** and **4** at physiological pH.

Overall, cyclic voltammetry confirmed the presence of two individual redox centres in **1–4**, both of which were under pH control. While the centres influenced each other, *e.g. via* electron

withdrawing effects, there was little enhancement or synergy between them. This was not surprising, as there was a substantial difference between the chalcogen and quinone redox potentials. Redox behaviour was further evaluated in bioassays indicative of redox catalysis.

Thiophenol and metallothionein peroxidation assays

Based on the electrochemical results, **2–4** in particular were expected to exhibit catalytic quinone and chalcogen redox behaviour *in vitro* (Fig. 3). The latter was measured in two independent assays; the thiophenol (PhSH) based glutathione peroxidase (GPx) assay[13] and the metallothionein (MT) assay.[14]

The PhSH assay is a simple catalytic assay measuring the peroxidation of PhSH by hydrogen peroxide (Table 2). The results obtained showed significant increases in the rate of PhSH oxidation in the presence of selenium and tellurium compounds **2–4**, with 13- to 25-fold increases over the control level (5.38 nM s^{-1}). In stark contrast, ebselen, used as a known benchmark, and the menadione **5** control showed no significant activity under the experimental conditions. Interestingly, the order of activity of **2–4** in the PhSH assay corresponded to the oxidation potential of the chalcogen (Epa_2), with **4** having the lowest Epa_2 value and highest activity and **2** having the highest potential and lowest activity.

The PhSH assay was complemented by the MT assay.[6] Compared to the PhSH assay, the latter is less prone to interference and can be carried out in buffered solution at pH 7.4 (avoiding the use of methanol as solvent). As would be expected for tellurium-based GPx mimics, **3** and **4** effectively enhanced cysteine protein oxidation in the presence of peroxide (Table 2). Compounds **1** and **2** had a similar, yet lower activity, in line with the results obtained in the PhSH assay and confirming a previously reported correlation between chalcogen oxidation potential and zinc release, and a generally lower activity of sulfur and selenium compounds when compared to their tellurium analogues.[11–15]

It should be noted that although the ranking of compounds is similar in the PhSH and MT assays, relative activities of compounds differ in the two assays. This is hardly surprising, since both assays employ significantly different parameters, such as different solvents, oxidants and thiol species.

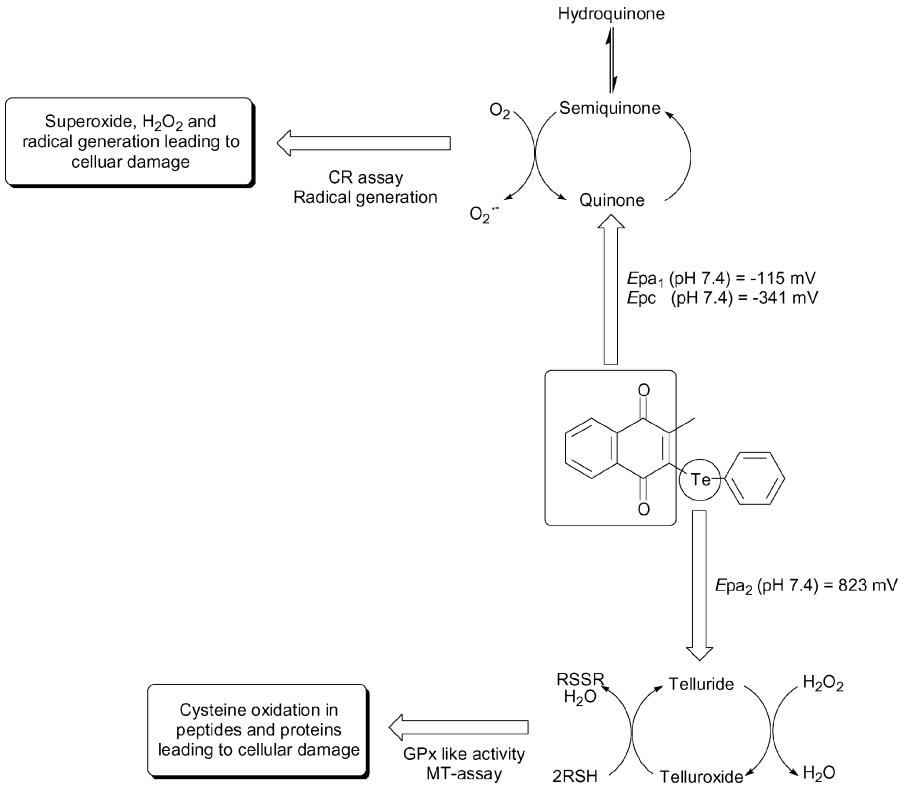

Fig. 3 Schematic view of the multifunctional properties of **1–4**, as illustrated on the most active compound **3**. Quinone-like radical generating activity, biologically important in *generating* oxidative stressors, has been indicated by the CR assay. GPx-like peroxidation catalysis, biologically important in *using* oxidative stressors to inflict cell damage, has been confirmed independently in the PhSH and MT assays.[6]

Table 2 Activity of **1–5** in protein-based *in vitro* assays. Chalcogen-based peroxidation activity is shown in the GPx and MT assays. The CR assay is indicative of quinone-based NADH consumption and superoxide generation in the presence of dioxygen. Together with the electrochemical findings, this information has been used to select compounds for testing in cell culture. Experimental details are given in the text

Compound	Initial reduction rate of H_2O_2 ±5%/10^{-9} Ms^{-1}	MT assay rate zinc release ±5%/10^{-10} Ms^{-1}[b]	Zinc release from MT after 60 min with BuOOH ±5% (%)[a]	CR rate/10^{-9} Ms^{-1}	CR number of turnovers after 2 h[c]
1	nd[a]	0.8	12	8.6	7.2
2	67	0.8	12	5.4	6.4
3	84	2.2	28	8.7	6.3
4	129	2.0	28	2.7	2.8
5	5	—	9	29.2	7.8
Ebselen	10	1.3	7	—	—

[a] Not determined. [b] Values have been corrected for background reaction, *i.e.* reaction without any test compound present. [c] Turnover numbers were established using the consumption of 1 mole eq. of NADH as 1 turnover. CR concentration in this assay was 6.5 μM.

Cytochrome C reductase assay for quinones

Redox activity of the quinone moiety was evaluated in the cytochrome C reductase (CR) assay. The results shown in Table 2 indicate that the quinone compounds are recognised as substrates by CR. Although there was some variation in activity, all compounds tested resulted in CR-catalysed oxidation of NADH. The initial rates observed for **1–4** were somewhat lower than the one of the parent menadione **5**, with **1** and **3** being the most active and **4** the least.

This assay also indicated that the quinones were acting as coenzymes in a coupled system with CR, as the consumption of NADH continued beyond the oxidation of 1 eq. of NADH per quinone in the presence of a 10-fold excess of NADH. Again, menadione **5** was most active, and consumed 8.6 eq. of NADH over a 120 min period (out of a theoretical maximum of 10). Similarly, sulfur compound **1** turned over 7.2 eq. of NADH, while **2** and **3** turned over 6.4 and 6.3 eq. of NADH, respectively. In line with the lowest initial rate observed among **1–5**, **4** only consumed 2.8 eq. of NADH over the 120 min period.

The oxidation of NADH beyond 1 mole eq. per quinone is incompatible with a stoichiometric oxidation, as only 2 electrons are required to fully reduce the quinone to the dihydroquinone. Rather, it suggests that the dihydroquinone moiety is not the final reduction product and that the reaction involves the generation of the superoxide radical anion, a process frequently observed for quinones such as plumbagin under aerobic conditions *in vitro* (Fig. 3).[6,16] Control incubations of CR with either NADH or catalysts individually showed no change in absorbance at 340 nm, neither did incubation of catalyst and NADH in the absence of CR.

Cytotoxicity in response to increased peroxide concentrations in PC12, Jurkat and Daudi cell lines

In order to evaluate the effect of the compounds on cells in the absence and presence of hydrogen peroxide, rat PC12, human Jurkat (J16) and human Daudi cell lines were chosen. These cell lines are representative of cancer cells that proliferate *in vivo* under OS conditions. Compound **3** was selected for these assays because it exhibited the highest activity in the MT and CR assay.

At low concentrations (100 nM), **3** was non-toxic to cultured PC12 cells that were not challenged by the addition of H_2O_2. In the presence of this oxidative stressor however, cell survival dramatically dropped to 45%.[6] While the parent quinone **5** also promoted cell death under oxidative stress conditions, a significantly higher concentration (3.2 μM) was required to obtain the same effect. Compound **3** was also far superior to 4,4′-dihydroxydiphenyl telluride, the most active GPx mimic studied earlier.[8] Administration of 10 μM of this compound reduced cell survival to 45%, whereas the same effect was observed for **3** at 100 nM concentration, an increase in efficacy of two orders of magnitude.

Selectivity for cells under OS was confirmed in the human Jurkat and Daudi cell lines (Fig. 4). For Jurkat cells exposed to 100 nM of **3** in the absence of H_2O_2 the survival observed was 67.4%, while the addition of 50 μM H_2O_2 (in itself not toxic at this concentration) decreased this to 27.8%, as shown in Fig. 4a. Compound **2** had a similar overall effect, where the survival of Jurkat cells was decreased from 115% to just 54.5% in the presence of 100 nM of this selenium compound. In contrast, **2** and **3** were not particularly toxic on their own, *i.e.* towards the cells *not* under OS, for catalyst concentrations below 1 μM (Fig. 4). Catalyst concentrations of 1 μM and above were toxic. A similar effect was observed for **3** in Daudi cells (Fig. 4b).

Overall, these cell culture experiments indicated that the catalysts (at low concentrations) reduced cell survival *in cells under OS*, but at these concentrations had little toxicity on their own, *i.e. in the absence of peroxide*. This effect was not limited to PC12 cells but instead seemed to be of a more general nature, although additional cell lines need to be considered before a full generalisation can be made.

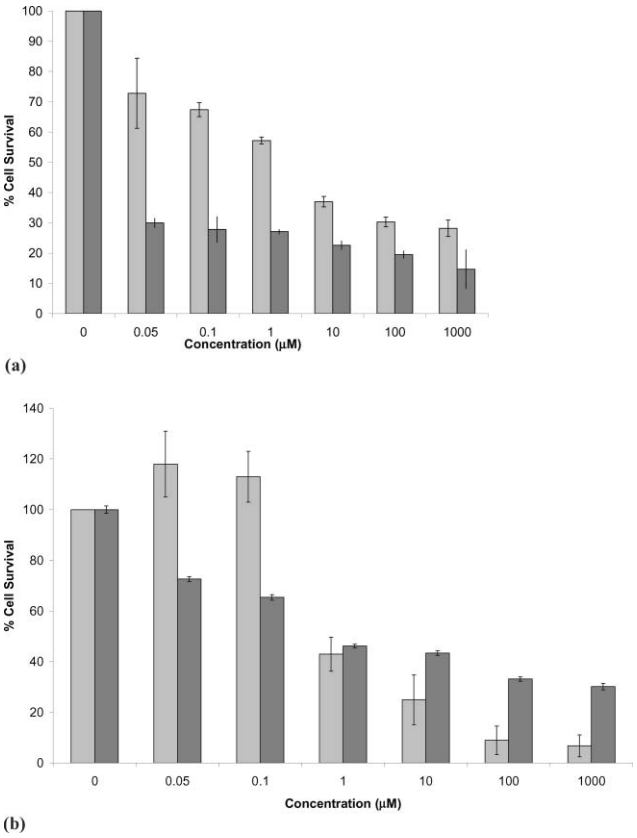

Fig. 4 Cytotoxicity assays for **3** in the absence (▒) and presence (■) of 50 μM H_2O_2. Fig. 4a show the results for human Jurkat and Fig. 4b for human Daudi cell culture. Experimental details are given in the text.

Preliminary mechanistic studies

The notion that catalysts like **3** might become toxic by increasing the severity of OS, either by generating additional ROS or by catalysing reactions with existing ROS, was then investigated in a series of preliminary mechanistic studies. It should be noted from the outset that the results obtained so far provide an indication of a likely mode of action, but not conclusive proof.

The 2,7-dichlorodihydrofluorescein acetate (DCDHF) assay was chosen to measure the overall levels of intracellular OS.[17–19] Although this assay is not specific for individual stressors and can be affected by hydrolysis of the dye, it is useful in obtaining an indication of intracellular stress levels during application of the catalysts. Fig. 5 shows the kinetic profile of oxidative stress generation in Jurkat and Daudi cells upon addition of **2** and **3**, as assessed by the formation of fluorescent carboxydichlorofluorescein from carboxydichlorodihydrofluorescein. This figure indicates that both compounds, in the absence of added peroxide, were able to significantly increase intracellular OS conditions inside the two cell lines over a 2 h period. In this respect, **2** and **3** had similar activity, with **3** being slightly more active than **2** in the Daudi cell line. In the Jurkat cell line, **2** increased fluorescence by 2.2-fold over the control, compared to 2.4-fold for **3** (Fig. 5a). In the Daudi cell line, **2** increased fluorescence by 1.6-fold over the control, compared to 2.1-fold for **3** (Fig. 5b).

In order to investigate the relationship between **3** and OS further, the monochlorobimane (MCB) method was used to estimate changes in intracellular levels of reduced glutathione (GSH). As with the DCDHF assay, this method is not without drawbacks but has been extensively used in the past to estimate GSH levels.[20–21] As expected for an enhancer of OS, **3** also caused a significant decrease of the intracellular GSH level in

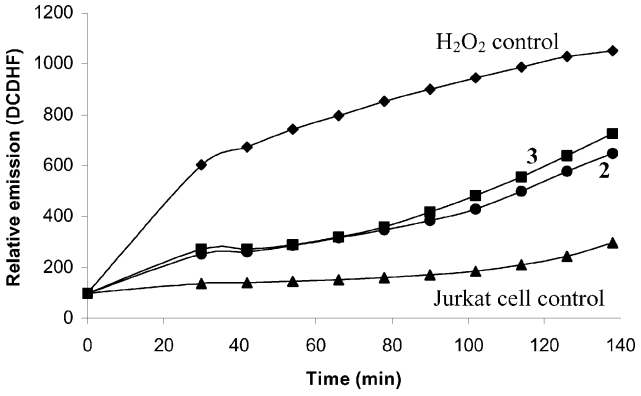

(a)

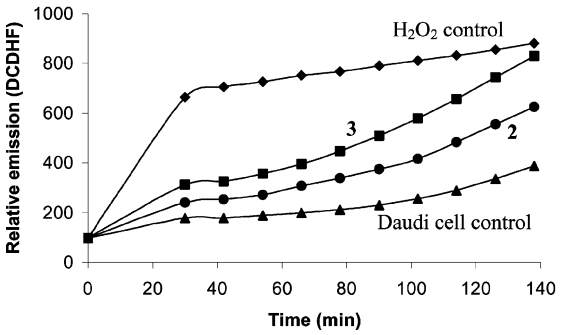

(b)

Fig. 5 Fluorescent DCDHF assays indicative of intracellular OS stress levels. Fig. 5a shows the results obtained for **2** and **3** in Jurkat cells and Fig. 5b in Daudi cells (both cell lines were treated with compounds in the absence of other external OS). In all cases, the basal OS stress level in untreated compounds and an increased OS stress level caused by added 50 μM H_2O_2 are given as negative and positive controls, respectively. Experimental error ±5%.

Jurkat cells to 59%. GSH depletion by **3** could be abrogated, however, by the addition of the antioxidant *N*-acetyl-L-cysteine (NAC). In these experiments, NAC slightly increased the GSH level to 125% of control and this level was then maintained in spite of the presence of **3**, supporting the notion that the **3** was acting *via* a redox pathway, rather than by inhibiting GSH synthesis. Further evidence of a link between **3**, increases in intracellular OS levels and apoptotic cell death was obtained using a combination of DCDHF, PI and DAPI staining in Jurkat and Daudi cells (results not shown). The precise mode of cell death is important for drug development and is currently being investigated in considerably more detail.

Discussion

Redox catalysts have the ability to influence intracellular redox processes, either as pro- or antioxidants.[7] Since catalysts rely on the presence of their substrates, such as ROS, for activity, they combine important sensor with effector functions that might be used to specifically target cells, such as cancer cells, under OS. The results presented here support the notion that catalysts develop selective toxicity in response to existing ROS.

Redox properties and pH control

The electrochemical results have confirmed the presence of two distinct redox couples in **1–4**. The quasi-reversible electrochemical behaviour of the quinone-moiety in these compounds, which is comparable to the one of the parent menadione **5**, points towards a similar biochemical activity of multi-functional compounds **1–4** and menadione. Within a biochemical context, the pH-dependency of this redox behaviour implies a higher radical generating activity of the quinone in regions of higher pH. This might become an important feature of these compounds, since increases of OS are frequently associated with changes in pH.

In contrast, the significant differences in the chalcogen oxidation potentials of **1–4** allow an electrochemical ranking, with compounds with the lowest Epa_2 values, *i.e.* **3** and **4** at around neutral pH, expected to exhibit the highest activity in the chalcogen-centred peroxidation assays (GPx and MT assays).

Peroxidation catalysis and superoxide generation *in vitro*

Building on the electrochemical studies, the catalytic *in vitro* assays have confirmed that **1–4** are multifunctional and can respond to different oxidative stressors. For example, the selenium and tellurium atoms in **2–4** form the centre for effective peroxidation (Fig. 3). Although the activity of compounds in the MT assay was generally reduced when compared to other, non-quinone selenium and tellurium catalysts, the two oxidation assays demonstrate the ability of these compounds to use peroxide in order to oxidise thiol proteins, *i.e.* to act as enhancers of OS. We have already shown that related catalysts are able to attack different, essential cysteine proteins, such as MT and zinc finger proteins,[8] and recent, independent studies have demonstrated the ability of similar chalcogen compounds to attack zinc finger proteins involved in DNA repair.[22]

The quasi-reversible, one and two electron transfer behaviour of the quinone moiety enables oxidation reactions. The reduced activity of **1–4** in the CR assay, when compared to **5**, might be explained by steric effects in the active site of CR, caused by the presence of the chalcogen atom and its attached phenyl ring system. The X-ray crystal structure of **3**‡ shows the close proximity of the tellurium atom and its phenyl ring system to the quinone redox centre, making a steric effect likely. The surprisingly high quinone-activity of sulfur compound **1**, when compared to the selenium and tellurium analogues, could therefore be due to a decrease in hindrance from tellurium to sulfur. Nevertheless, electronic effects, which also change from sulfur to tellurium, cannot be ruled out.

As mentioned above, the consumption of excess of NADH, ranging from 7.2 mole eq. for **1** to 2.8 mole eq. for **4** within 120 min, implies that CR-catalysed quinone reduction to dihydroquinone cannot be the only redox process in the assay. The turnover numbers observed in the CR assay should therefore be tentatively interpreted as a coupled redox process, where dioxygen re-oxidises the semi- or dihydroquinone (Fig. 3). Such a process, which is well known for menadione **5**, results in the formation of the superoxide radical anion and hydrogen peroxide.[6,23] The latter might be used as substrate by the chalcogen moiety of the compound. Although further studies of the quinone moiety would be required for a deeper interpretation of these results, radical generation might play a major role in the biological activity of **1–4**. Superoxide, or some of its metabolic products (*e.g.* hydroxyl radicals), can lead to serious cell damage, especially in cells already under OS or with an impaired antioxidant defence.

The presence of two or more independent redox sites, each of which can be fine-tuned in its activity, is a characteristic important for the future development of potential catalytic drugs. Additional functional groups, such as metal binding sites or an amine anchor for attachment to transport proteins, might also be included into the design and added with comparable ease.[24–25]

Enhancement of OS in Jurkat and Daudi cells

In the light of the electrochemical and *in vitro* findings, it is hardly surprising that the activity of **3** in cell culture also points towards intracellular processes involving oxidative stressors. We have recently shown that the toxicity of such compounds is significantly increased in the presence of H_2O_2.[8] The results presented here show that this effect is not limited to cultured

rat PC12 cells, but can also be observed in other cell types, such as human Jurkat and Daudi cells.

The mechanistic studies, although of a preliminary nature, support the notion that **3** and, to a somewhat lesser extent, **2** are able to aggravate OS in the Daudi and Jurkat cell lines. This effect is likely to be the result of quinone-based superoxide formation (the latter will be metabolised by superoxide dismutase enzymes to H_2O_2 and dioxygen) and peroxidation catalysis that greatly enhances the physiological impact of H_2O_2.[26] The link between the catalysts and an intracellular increase of OS is also reflected by a significant decrease in GSH levels in the MCB assay, with GSH a major determinant of redox status in mammalian cells.

Considered together, the biochemical findings support the notion of a catalytic generation or conversion of ROS that leads to cell damage and ultimately cell death, probably *via* an apoptotic process. An apoptotic mode of cell death is not too surprising in this context, since hydrogen peroxide induced stress has already been linked to apoptosis in PC12 and Jurkat cells.[27–28] Although it is difficult at this point to determine an exact mechanistic relationship between the compounds and cell death, modulation of underlying redox processes provides a good working hypothesis (Fig. 6).

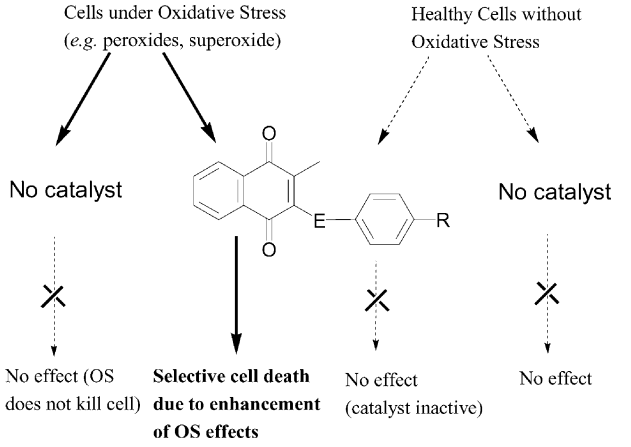

Fig. 6 Proposed mechanism by which redox catalysts cause selective cell death. This working model shows the sensing ability of catalysts and the aggravation of intracellular OS conditions that favour cell death *via* an apoptotic process.

Since natural, physiological levels of H_2O_2 and other ROS vary greatly between healthy and diseased cells, the synergistic effects between these stress markers and the catalysts provide a reasonable degree of specificity. This is particularly interesting in the context of cancer research, since the intracellular redox state of some cancer cells is more oxidizing compared to healthy cells and apoptosis would be a preferred mode of cancer cell death. Interestingly, recent work on the selective cytotoxicity of superoxide dismutase mimics has led to similar results, supporting the possible use of catalysts in cancer therapy.[29]

Based on the chemistry of the catalytic process, it is likely that most cell types under OS will be affected. This implies that other cells suffering from OS, such as inflammatory cells, might also be affected by the compounds. Further cell culture studies are therefore required to determine how widely applicable the catalytic effects observed here are. Such studies will also be able to shed more light on the exact mode of action of the compounds inside cells.

Conclusions

Compounds that aggravate, rather than simply generate physiological conditions such as OS, are able to sense intracellular conditions of existing OS and use these markers to affect cell survival. In theory, this sensor–effector combination provides an elegant, catalytic approach towards drug design. The studies presented here lend experimental support to this notion by presenting compounds that are more cytotoxic to oxidatively stressed cells than to cells under normal redox conditions. They also show that it is possible to use chemical design criteria, such as electronic effects and the combination of individual catalytic centres in one molecule, to obtain highly active catalysts with the expected activities.

More thorough biochemical and *in vivo* investigations are now underway to determine the precise mode of action of the compounds and possible metabolic conversions. These studies also need to address the complex redox behaviour seen for compounds such as **2–4** *in vitro*. Ultimately, animal testing will be required to evaluate efficiency, toxicity and to study pharmacokinetic parameters. On the other hand, the notion of catalysts as biochemical sensor–effector compounds is not limited to **1–4** and a wide range of multifunctional catalysts, with two or even more redox centres combined in chemically simple molecules, is possible. The work presented here should therefore be seen as providing the impetus for follow-on investigations, including synthetic chemistry and cell biology.

Experimental

Materials

Buffers, thiol reagents, methanol, hydrogen peroxide, catalase (bovine liver), cytochrome C reductase (porcine heart), *N*-acetyl-L-cysteine (NAC), propidium iodide (PI), 4′,6-diamidino-2-phenylindole (DAPI), 2,7-dichlorodihydrofluorescein acetate (DCDHF), $ZnSO_4$ (99.999%), and 2-methyl-1,4-naphthoquinone (**5**) were purchased from Sigma-Aldrich (Poole, UK). Tissue culture grade phosphate buffered saline (PBS), foetal bovine serum, L-glutamine, trypsin and gentamicin were purchased from Gibco (Paisley, UK) or BioWhittaker™ (Berkshire, UK). RMPI 1640 medium with and without Phenol Red, horse serum, nutrient mixture F-12 HAM medium, fibronectin, water, endothelial cell growth supplement and heparin were all purchased from Sigma-Aldrich or BioWhittaker™. All commercial chemicals were analytical or cell culture grade and needed no further purification. Solutions and buffers were prepared in MilliQ water and nitrogen flushed prior to use. Cd,Zn-metallothionein was purchased from Sigma and Zn_7–MT was reconstituted and purified according to a standard method.[30] Rat adrenal phaeochromocytoma PC12 cell lines were obtained from the European Collection of Cell Cultures (ECACC, No. 88022401). The human T-lymphoblastic leukaemia Jurkat J16 cell line and the human Epstein–Barr virus positive B-lymphoblastoid Daudi cell line were kind gifts from Dr C. Pourzand, University of Bath, UK and Dr H. Martin, University of Bristol, UK, respectively.

UV–Vis spectra were recorded on a CARY 50*Bio* spectrophotometer (Varian). Cyclic voltammetry was performed on a 100B/W workstation (BAS). Cells were incubated in a Sanyo CO_2 incubator and cell viability measured using either a Dynex technologies MRX microplate reader (MTT assays) or an EL800 Universal Microplate Reader from Bio-Tek Instruments Inc. (sulforhodamine B assays). Fluorescent microscopy was performed using a Carl Zeiss Axioskop2 Mot Plus microscope with imaging software Axio Vision. A FLUOstar OPTIMA fluorescent microplate reader, kindly provided by BMG Lab Technologies, UK, was used for the measurements of intracellular levels of OS. A Spectronic unicam Aminco Bowman Series 2 Luminescence spectrometer was used for the MCB assay.

Methods

The redox catalysts were synthesised and studied with a combination of chemical, biochemical and cell culture assays to evaluate their redox behaviour, interactions with proteins, cytotoxicity against cells in the absence/presence of OS and possible mode of action inside cells. Unless stated otherwise,

all experiments described (except synthetic chemistry) were performed in triplicate.

Synthesis of compounds

2-Methyl-3-bromo-1,4-naphthoquinone was synthesised according to an established procedure.[31] Compound **2** was synthesised using an analogous procedure to that outlined by Sakakibara *et al.*[32] using 2-methyl-3-bromo-1,4-naphthoquinone as the starting reagent (Fig. 1).

2-(Phenylsulfuryl)-3-methyl-[1,4]naphthoquinone (1). The reaction was performed under argon and in the dark (flask wrapped in foil). Absolute ethanol was degassed with argon for 30 min prior to use. 4,4′-dimethoxydiphenyl disulfide (748 mg, 2.69 mmol) was dissolved in absolute ethanol (15 ml). $NaBH_4$ (193 mg, 5.105 mmol) was added to the stirring solution, which turned colourless. This was allowed to stir for 20 min. 2-Bromo-3-methyl-[1,4]naphthoquinone (1.079 g, 4.30 mmol) was added, which turned the mixture dark red immediately. Stirring continued for 3 h, after which time the solvent was removed. The resulting brown solid was purified on a silica column eluting the orange product with 50% Et_2O–pet. Reducing the solvent and leaving the solution stand at −20 °C for 48 h produced orange crystals. Yield 32 mg (2%). ^{1}H NMR (300 MHz, $CDCl_3$): δ 8.07 (m, 1H), 7.99 (m, 1H), 7.67 (m, 2H), 7.38 (m, 2H), 6.83 (m, 2H), 3.78 (s, 3H), 2.31 (s, 3H). ^{13}C NMR ($CDCl_3$) δ 182.99, 180.72, 159.41, 147.35, 146.44, 133.55, 133.44, 131.97, 126.84, 126.44, 123.90, 114.70, 55.25, 15.57. Elemental analysis: calcd for $C_{17}H_{12}O_2S$: C 69.66; H 4.55%. Found: C 69.48; H 4.85%. Electronic spectra λ_{max}(MeOH)/nm (ε/dm^3 mol^{-1}cm^{-1}): 426 (1700), 332 sh (3250), 252 (26 460), 203 (47 800).

2-(Phenyltelluryl)-3-methyl-[1,4]naphthoquinone (3). Compound **3** was synthesised in exactly the same manner as described directly above using 4,4′-diphenyl ditelluride (107 mg, 0.26 mmol) and 2-bromo-3-methyl-[1,4]naphthoquinone (137 mg, 0.55 mmol). The resulting purple solid was purified on a silica column, eluting the starting telluride with 7% Et_2O–pet and eluting the purple product with 10% Et_2O–pet. Reducing the solvent and leaving the solution stand at −20 °C for 48 h produced dark purple crystals suitable for X-ray diffraction studies. Yield 17 mg (9%). ^{1}H NMR (300 MHz, $CDCl_3$) δ 8.02 (m, 2H), 7.78 (m, 2H), 7.63 (m, 2H), 7.30 (m, 1H), 7.20 (m, 2H), 1.90 (s, 3H). ^{13}C NMR ($CDCl_3$) δ 184.29, 181.27, 153.48, 142.11, 139.72, 139.56, 139.42, 133.82, 133.28, 131.99, 131.57, 129.54, 127.08, 126.95, 114.23, 20.19. Elemental analysis: calcd for $C_{17}H_{12}O_2Te$: C 54.32; H 3.22%. Found: C 54.08; H 3.04%. Electronic spectra λ_{max}(MeOH)/nm (ε/dm^3 mol^{-1}cm^{-1}): 517 (1100), 326 sh (2806), 269 sh (12 060), 240 sh (20 400), 221 sh (23 000), 204 (38 150).

2-(4-Methoxy-phenyltelluryl)-3-methyl-[1,4]-naphthoquinone (4). Compound **4** was synthesised in exactly the same manner as described directly above using 4,4′-dimethoxydiphenyl ditelluride (514 mg, 1.09 mmol) and 2-bromo-3-methyl-[1,4]naphthoquinone (575 mg, 2.29 mmol). Yield 332 mg (75%). ^{1}H NMR (300 MHz, $CDCl_3$) δ 8.06 (m, 2H), 7.78 (m, 2H), 7.68 (m, 2H), 6.80 (m, 2H), 3.83 (s, 3H), 1.92 (s, 3H). ^{13}C NMR ($CDCl_3$) δ 184.56, 181.27, 160.29, 153.13, 142.19, 141.87, 133.77, 133.20, 132.02, 131.59, 126.98, 126.92, 115.44, 103.33, 55.16, 19.39. Elemental analysis: calcd for $C_{18}H_{14}O_3Te$: C 53.26; H 3.48%. Found: C 53.32; H 3.40%. Electronic spectra λ_{max}(MeOH)/nm (ε/dm^3 mol^{-1}cm^{-1}): 517 (1275), ~325 sh (2730), ~271 sh (10 800), 243 (25 900), 204 (37 500).

X-Ray measurement of 3

Crystal data. $C_{17}H_{12}O_2Te$, M = 375.87, monoclinic, a = 11.8427(9), b = 6.0131(3), c = 20.0259(11) Å, β = 90.914(5)°, U = 1425.89(15) Å^3, T = 120 K, space group $P2_1/n$ (no. 14), Z = 4, μ(Mo–Ka) = 2.084 mm^{-1}, 9936 reflections measured, 2793 unique (R_{int} = 0.046) which were used in all calculations. The final $wR(F^2)$ was 0.0849 (all data).‡

Cyclic voltammetry

Cyclic voltammograms of organochalcogens (50–100 μM) were recorded in potassium phosphate buffer (50 mM) containing 30% methanol, due to the limited solubility of the organochalcogens in aqueous media. The pH range included pH 4, 5, 6, 7.4, 8 and 9. A standard Ag/AgCl reference electrode (SSE) and a glassy carbon (GCE) working electrode were used, with an internal ferrocene reference standard to compensate eventual changes in SSE potential. Counter and working electrode were thoroughly cleaned and polished (Al_2O_3) after each scan. Cyclic voltammograms were recorded at scan rates between 100 to 500 mV s^{-1}. The potential range was between −600 mV to +1400 mV *vs.* SSE.[6–7]

Protein assays

Thiophenol peroxidation assay. The thiophenol oxidation assay (PhSH) is a spectrophotometric assay that measures GPx-like catalytic activity by monitoring the formation of PhSSPh from PhSH in the presence of hydrogen peroxide.[13] Briefly, 100 μM of compound was added to a 1 mM methanolic solution of PhSH, the reaction initiated by addition of 2 mM H_2O_2 and monitored at 305 nm for 20 min at 25 °C. Initial rates were obtained for the interval of 1 and 2 min.

Metallothionein zinc release assay. Since the PhSH assay is frequently disturbed (*e.g.* if coloured catalysts are used), the more robust and also biologically more relevant metallothionein (MT) zinc release assay was used to complement the PhSH assay.[14,33] This assay measures the ability of agents to catalyse the reaction of *tert*-butyl hydroperoxide (*t*-BuOOH) with the biologically abundant zinc–sulfur protein MT, whose zinc ions are released upon oxidation of the protein's cysteine ligands; a process that can be monitored spectrophotometrically in the presence of a Zn^{2+} binding dye. In these assays, MT (0.5 μM) was incubated with *t*-BuOOH (500 μM) and 4-(2-pyridylazo)-resorcinol monosodium salt (PAR, 100 μM) in 20 mM Na^+–HEPES buffer (pH 7.4, 25 °C) in the absence and presence of various concentrations of catalysts. Compounds were evaluated according to the initial rate of zinc release and the total extent of zinc release after 60 min. Maximum zinc release was measured using ebselen as standard and activities are expressed as a percentage of this value.

Cytochrome C reductase assay. To characterise and quantify the prospective oxidant effects of the quinone moiety of each catalyst an assay was established based on the ability of the compounds to function as a coenzyme for porcine heart cytochrome C reductase (CR).[34] CR is a widely promiscuous enzyme, which catalyses the reduction of a variety of substrates by NADH and therefore serves as a model for the interactions of the compounds with redox enzymes within the cell. CR (5 μM), NADH (500 μM) and compound (50 μM), were incubated together in 10 mM phosphate buffer, pH 7.5, for 10 min. By monitoring at 340 nm, the rate at which NADH was oxidised to NAD^+ was derived from the slope of the kinetic trace.

Cell culture

Cell culture tests were performed in the following cell lines: rat PC12 cells, human Jurkat (J16) and human Daudi cells. Undifferentiated PC12 cells were cultured in suspension in RPMI 1640 supplemented with 2 mM L-glutamine, 10% horse serum, 5% heat inactivated foetal bovine serum and 250 U per ml gentamicin at 37 °C, 5% CO_2 and 95% air.[35] For experimentation, undifferentiated cells were plated at 10^5 cells per well into 96 well tissue culture plates.

The Jurkat and Daudi cell lines were maintained in RPMI 1640 medium supplemented with 10% heat inactivated foetal bovine serum, 2 mM L-glutamine, 100 U per ml penicillin, and 100 μg ml^{-1} streptomycin at 37 °C, 5% CO_2 and 95% air. Cells of no lower than 90% viability as determined by the trypan blue exclusion assay were used. For all experimentation, cells were plated at 10^4 cells per well in phenol red free medium supplemented with 10% heat inactivated foetal bovine serum, 2 mM L-glutamine, 100 U per ml penicillin and 100 μg ml^{-1} streptomycin.

Measurement of cell survival by the MTT assay

Cell viability of PC12 cells was measured using the MTT (3-[4,5-dimethylthiazol-2-yl]-2,5-diphenyltetrazolium bromide) assay.[36] MTT (0.5 mg ml^{-1}, in PBS) was added to the 96 well plate (final concentration, 0.1 mg ml^{-1}) and incubated for a period of 3 h. The reduced MTT crystals were solubilised in 30% DMSO and the colourimetric evaluation of reduced MTT was determined spectrophotometrically at 540 nm.

In order to test the activity of compounds on PC12 cell survival, cells were plated and then pre-incubated for 1 h with varying concentrations (1 nM–25 μM) of catalyst **3** at 37 °C, 5% CO_2 and 95% air, followed by the addition of H_2O_2 (200 μM) and overnight incubation. In a separate experiment, cells were pre-incubated with **3** (10 μM) followed by addition of varying H_2O_2 concentrations (50–500 μM). A H_2O_2 dose response curve in the absence of catalyst was established as a control (data not shown). In addition, analogue experiments were performed with the chalcogen-free, parent quinone **5** as a control. All compounds were initially solubilised in methanol and diluted in medium to the appropriate concentration with 2% methanol to maintain solubility. Methanol and also catalyst alone (no H_2O_2) were incubated as established controls. Cell viability was expressed as a percentage of normal growth (in absence of compounds and H_2O_2). Individual treatments consisted of six wells per experiment, of which experiments were replicated at least four times and presented as an average (mean ± S.D.).

Sulforhodamine B cytotoxicity assay

Jurkat and Daudi cells growing in log phase were incubated at the required concentration (10^4 cells per well) in 96-well microplate with or without a bolus injection of 50 μM H_2O_2. The sulforhodamine B (SRB) assay was performed following an established literature method.[37] Briefly, the cells were incubated with the compounds for 4 days and the cultures were then fixed with ice cold 50% TCA and stained with 0.4% SRB dissolved in 1% acetic acid. After dissolving the bound cells with 100 μl of 10 mM unbuffered aqueous Tris base (pH 10.5) using a gyratory shaker, the absorbance at 490 nm was determined. Binding of SRB dye to basic amino acids has a linear relationship with cell density and SRB staining serves as an accurate method in measuring cell density through total protein staining.[38]

Fluorescent assay indicative of intracellular ROS concentrations

Within limits, the oxidizing environment inside cells can be estimated using 2,7-dichlorodihydrofluorescein acetate (DCDHF). This compound readily enters cells, where it is cleaved by non-specifice esterases to carboxydichlorodihydrofluorescein. When oxidised by ROS (*e.g.* H_2O_2), fluorescent carboxydichlorofluorescein is formed that can be quantified as a measure of intracellular OS.

Jurkat and Daudi cells were seeded in 96 wells plates at a density of 10^4 cells per well in phenol red-free RPMI 1640 medium and compounds (10 μM) and/or H_2O_2 (50 μM) were added as a bolus injection. Cells were incubated for a further 30 min. DCDHF (10 μM) was then added to the cell culture medium and allowed to incubate for 30 min in the dark, at 37 °C, in 5% CO_2 and 95% air. Fluorescence was then monitored with the microplate fluorimeter, using an excitation wavelength of 485 nm and an emission wavelength of 538 nm.

Monochlorobimane GSH assay indicative of intracellular GSH concentrations

The MCB assay is fairly specific for GSH and allows the determination of GSH concentrations in the presence of other intracellular thiols. The assay was based on a literature procedure,[20–21] with the following modifications: after treating cells with or without 10 μM compounds and with or without 200 mM *N*-acetyl-L-cysteine (NAC) for 24 h, samples of 10^6 cells were resuspend in 2 ml of PBS containing 50 μM MCB and incubated for 30 min in the dark at rt. A 1 ml aliquot of the cell suspension was transferred into a fluorescent cuvette and fluorescence emission measured at an excitation wavelength of 395 nm and an emission wavelength of 482 nm. PBS incubated with 50 μM MCB was used as control. Means of % GSH compared to the untreated control sample were calculated (as an average of two samples).

Acknowledgements

This work was financially supported by the Wellcome Trust, the Leverhulme Trust, DAART, Exeter Antioxidant Therapeutics Ltd. and the University of Exeter (UK). C. J. acknowledges a Visiting Professorship from the Université de Metz (France). The authors are grateful to Prof. Winyard (Exeter) and Prof. Kirsch (Metz) for helpful discussions and wish to thank BMG for the use of their fluorescent microplate reader. The also acknowledge Drs Pourzand (Bath) and Martin (Bristol) for donating cell cultures.

References

1 T. D. Oberley and L. W. Oberley, *Histol. Histopathol.*, 1997, **12**, 525–535.
2 D. B. Coursin, H. P. Cihla, J. Sempf, T. D. Oberley and L. W. Oberley, *Histol. Histopathol.*, 1996, **11**, 851–860.
3 W. Droge, *Physiol. Rev.*, 2002, **82**, 47–95.
4 A. Keshavarzian, A. Banan, A. Farhadi, S. Komanduri, E. Mutlu, Y. Zhang and J. Z. Fields, *Gut*, 2003, **52**, 720–728.
5 Z. A. Massy and T. Nguyen-Khoa, *J. Nephrol.*, 2002, **15**, 336–341.
6 G. I. Giles, N. M. Giles, C. A. Collins, K. Holt, F. H. Fry, P. A. S. Lowden, N. J. Gutowski and C. Jacob, *Chem. Commun.*, 2003, 2030–2031.
7 N. M. Giles, N. J. Gutowski, G. I. Giles and C. Jacob, *FEBS Lett.*, 2003, **535**, 179–182.
8 N. M. Giles, G. I. Giles, J. E. Holley, N. J. Gutowski and C. Jacob, *Biochem. Pharmacol.*, 2003, **66**, 2021–2028.
9 S. Bali, A. K. Singh, P. Sharma, R. A. Toscano, J. E. Drake, M. B. Hursthouse and M. E. Light, *J. Organomet. Chem.*, 2004, **689**, 2346–2353.
10 L. Engman, I. Kania, B. J. Oleksyn, J. Sliwinski and A. Wojton, *J. Mol. Struct.*, 2002, **609**, 47–54.
11 G. I. Giles, K. M. Tasker, R. J. K. Johnson, C. Jacob, C. Peers and K. N. Green, *Chem. Commun.*, 2001, 2490–2491.
12 L. Engman, D. Stern, I. A. Cotgreave and C. M. Andersson, *J. Am. Chem. Soc.*, 1992, **114**, 9737–9743.
13 M. Iwaoka and S. Tomoda, *J. Am. Chem. Soc.*, 1994, **116**, 2557–2561.
14 C. Jacob, W. Maret and B. L. Vallee, *Biochem. Biophys. Res. Commun.*, 1998, **248**, 569–573.
15 G. I. Giles, F. H. Fry, K. M. Tasker, A. L. Holme, C. Peers, K. N. Green, L.-O. Klotz, H. Sies and C. Jacob, *Org. Biomol. Chem.*, 2003, **1**, 4317–4322.
16 S. Baez, Y. Linderson and J. Segura-Aguilar, *Biochem. Mol. Med.*, 1995, **54**, 12–18.
17 R. Cathcart, E. Schwiers and B. N. Ames, *Anal. Biochem.*, 1983, **134**, 111–116.
18 J. A. Scott, C. J. Homcy, B. A. Khaw and C. A. Rabito, *Free Radical Biol. Med.*, 1988, **4**, 79–83.
19 G. Melino, I. Savini, P. Guerrieri and A. Finazziagro, *Free Radical Res. Commun.*, 1990, **11**, 213–221.
20 J. Sebastia, R. Cristofol, M. Martin, E. Rodriguez-Farre and C. Sanfeliu, *Cytometry*, 2003, **51A**, 16–25.
21 D. W. Hedley, A. R. Hallahan and E. H. Tripp, *Br. J. Cancer*, 1990, **61**, 65–68.

22 H. Blessing, S. Kraus, P. Heindl, W. Bal and A. Hartwig, *Eur. J. Biochem.*, 2004, **271**, 3190–3199.
23 W. G. Rice, C. D. Hillyer, B. Harten, C. A. Schaeffer, M. Dorminy, D. A. Lackey, 3rd, E. Kirsten, J. Mendeleyev, K. G. Buki and A. Hakam, *et al.*, *Proc. Natl. Acad. Sci. USA*, 1992, **89**, 7703–7707.
24 S. Pariagh, K. M. Tasker, F. H. Fry, A. L. Holme, C. A. Collins, N. Okarter, N. Gutowski and C. Jacob, *Org. Biomol. Chem.*, 2005, **3**, 975–980.
25 C. A. Collins, F. H. Fry, A. L. Holme, A. Yiakouvaki, A. Al-Qenaei, C. Pourzand and C. Jacob, *Org. Biomol. Chem.*, 2005, **3**, 1541–1546.
26 N. M. Giles, A. B. Watts, G. I. Giles, F. H. Fry, J. A. Littlechild and C. Jacob, *Chem. Biol.*, 2003, **10**, 677–693.
27 H. Kim, Y.-N. Kim, H. Kim and C.-W. Kim, *Oncogene*, 2005, **24**, 1252–1261.
28 B. Jiang, J. H. Liu, Y. M. Bao and L. J. An, *Cell Biol. Int.*, 2003, **27**, 1025–1031.
29 N. Kasugai, T. Murase, T. Ohse, S. Nagaoka, H. Kawakami and S. Kubota, *J. Inorg. Biochem.*, 2002, **91**, 349–355.
30 M. Vašák, *Methods Enzymol.*, 1991, **205**, 41–44.
31 R. Adams, T. A. Geissman, B. R. Baker and H. M. Teeter, *J. Am. Chem. Soc.*, 1941, **63**, 528–534.
32 M. Sakakibara, Y. Watanabe, T. Toru and Y. Ueno, *J. Chem. Soc., Perkin Trans. 1*, 1991, 1231–1234.
33 C. Jacob, W. Maret and B. L. Vallee, *Proc. Natl. Acad. Sci. USA*, 1999, **96**, 1910–1914.
34 P. David, M. Baumann, M. Wikstrom and M. Finel, *Biochim. Biophys. Acta*, 2002, **1553**, 268–278.
35 S. Kearns and R. Dawson, Jr., *Adv. Exp. Med. Biol.*, 2000, **483**, 563–570.
36 E. K. Jaffe, R. L. Nachman, C. G. Becker and C. R. Minick, *J. Clin. Invest.*, 1973, **52**, 2745–2456.
37 P. Skehan, R. Storeng, D. Scudiero, A. Monks, J. McMahon, D. Vistica, J. T. Warren, H. Bokesch, S. Kenney and M. R. Boyd, *J. Natl. Cancer Inst.*, 1990, **82**, 1107–1112.
38 K. Haselsberger, D. C. Peterson, D. G. Thomas and J. L. Darling, *Anti-Cancer Drugs*, 1996, **7**, 331–338.